

Modelling of Solid Wall Boundaries in Computational Acoustics

R. C. Z. Cohen, A. Ooi and R. Widjaja

Department of Mechanical & Manufacturing Engineering
The University of Melbourne, VIC, 3010 AUSTRALIA

Abstract

This paper details an investigation into the Impedance Mismatch Method (IMM) as a means of modelling solid-wall boundaries for both one- and two-dimensional computational aeroacoustics (CAA) simulations. The main attraction of this method is its ability to model curved shaped bodies on a cartesian grid. Firstly, the IMM is used to model a solid wall within a one dimensional domain. In its given form the IMM is seen to allow the transmission of small acoustic waves through the solid region. A modification involving damping within the solid region is shown to be an effective improvement. The modified IMM was also used to simulate acoustic scattering off a rectangular block. The results compare well with those obtained using the Tam and Dong wall boundary technique.

Introduction

Computational aeroacoustics (CAA) is a subfield of computational fluid dynamics (CFD) that has seen rapid growth over the past decade. This has been primarily due to the development of algorithms for the spatial and temporal discretizations of the governing equations that have minimal numerical dispersion and dissipation errors. In this investigation many of the more recent numerical techniques are employed in the investigation of different solid wall boundary modelling. In general, the governing equations of acoustics are the compressible Navier–Stokes equations. However, for the acoustic field, viscous effects are usually neglected, so the Euler equations can be used. The linearized, nondimensionalized Euler equations with a mean flow Mach number of M in the x -direction are given by:

$$\frac{\partial U}{\partial t} + [A] \frac{\partial U}{\partial x} + [B] \frac{\partial U}{\partial y} = 0 \quad (1)$$

where:

$$U = \begin{bmatrix} \rho \\ u \\ v \\ p \end{bmatrix} \quad [A] = \begin{bmatrix} M & 1 & 0 & 0 \\ 0 & M & 0 & 1 \\ 0 & 0 & M & 0 \\ 0 & 1 & 0 & M \end{bmatrix} \quad [B] = \begin{bmatrix} 0 & 0 & 1 & 0 \\ 0 & 0 & 0 & 0 \\ 0 & 0 & 0 & 1 \\ 0 & 0 & 1 & 0 \end{bmatrix}$$

Numerical Methods

The following subsections detail the numerical methods that are used in this investigation.

Time and Spatial Discretization

A standard 4th order accurate Runge-Kutta time marching scheme is used in this investigation. Small time steps are used to avoid issues of temporal dispersion error. Explicit finite difference schemes for spatial derivatives are generally given in the form:

$$\left(\frac{\partial f}{\partial x} \right)_i \simeq \frac{1}{\Delta x} \sum_{j=-N}^M a_j f_{i+j} \quad (2)$$

where a_j are the coefficients of the particular scheme. For CFD calculations, such coefficients are typically chosen to satisfy some formal accuracy of the Taylor series expansions.

In CAA however, the dispersion relation of the discretization scheme is of equal importance to the formal accuracy. Tam and Webb [9] developed the so called Dispersion Relation Preserving (DRP) finite difference scheme that uses a wide stencil with some coefficients chosen to minimise the dispersion error. This scheme has higher resolution than standard central differencing schemes, allowing the use of less gridpoints per wavelength in order to achieve the required accuracy. Both the central and one sided 4th order DRP coefficients used in this investigation are given by Tam [5].

Absorbing Boundary Layer

The infinite physical domain is necessarily modelled on a finite computational grid. This requires the introduction of absorbing boundary conditions that allow outgoing waves to exit the computational grid without reflection. One method that achieves this is known as the Perfectly Matched Layer (PML) technique of Hu [3]. This methodology employs a buffer region at the edge of the grid that theoretically perfectly absorbs waves of all frequencies independent of the angle of incidence. Further development by Hu led to a more stable formulation [2] that also doesn't require the physical variables to be split as done in earlier versions. It is this formulation that is used in the study.

Solid Wall Boundaries

In the literature there are two methods of treating solid wall boundaries. Tam and Dong [7] discussed wall boundary conditions for computational acoustics. They concluded that the main physical wall boundary conditions to be implemented are:

$$v_n = 0 \quad (3)$$

$$\frac{\partial p}{\partial n} = 0 \quad (4)$$

That is, the fluid velocity normal to the wall is zero and the pressure gradient normal to the wall is zero. To implement these conditions, one sided and partially one sided stencil coefficients for the spatial derivatives were developed. The initial value of the velocity normal to the wall is explicitly set to zero. A row of ghost points for pressure are added inside the wall. The values of these ghost pressures are continuously set to ensure the pressure gradient at the wall is zero.

Chung and Morris [1] developed the so called Impedance Mismatch Method (IMM) for modelling solid wall boundaries. In this scheme each point on a cartesian grid is assigned a mean density ρ and a sound speed a . The solid wall is modelled with a markedly different characteristic impedance (ρa) to that of the fluid region. Curved solid bodies may be adequately modelled by assigning grid points as either inside or outside the body. At the interface between two regions waves are perfectly reflected if the impedance ratio is infinite. Due to instabilities that arise in having a ratio that is too large, the finite impedance ratio they recommend to use is around $1/30$. According to Laik and Morris [4], the amplitude of the reflected wave (p_r) to the incident

wave (p_i) is given by:

$$R = \left| \frac{p_r}{p_i} \right| = \frac{\rho_2 a_2 - \rho_1 a_1}{\rho_1 a_1 + \rho_2 a_2} \quad (5)$$

where ρ_1 and ρ_2 are the mean densities and a_1 and a_2 are the speeds of the sound in the two media. IMM requires the reformulation of the Euler equations to include the density terms inside the spatial derivative operators. The density in the acoustic regions of the grid is set to unity and inside the solid wall regions it is set to a much smaller value, depending on the particular density ratio to be used. The following are the two dimensional IMM Euler equations with mean flow Mach number M in the x direction:

$$\frac{\partial U}{\partial t} + \frac{\partial E}{\partial x} + \frac{\partial F}{\partial y} = 0 \quad (6)$$

where:

$$U = \begin{bmatrix} \rho \\ u \\ v \\ p \end{bmatrix} \quad E = \begin{bmatrix} M\rho + \rho_0 u \\ Mu + p/\rho_0 \\ Mv \\ Mp + \rho_0 u \end{bmatrix} \quad F = \begin{bmatrix} \rho_0 v \\ 0 \\ p/\rho_0 \\ \rho_0 v \end{bmatrix}$$

Artificial Selective Damping

Solid wall boundaries, especially ones with sharp edges often result in spurious waves being generated. Due to the limited resolution of finite difference schemes these waves will travel at supersonic speeds and contaminate the solution. Tam and Dong [6] studied these short wave components and developed an artificial selective damping technique that can be used to remove these high frequency waves from the calculations. Tam and Shen [8] improved this with a variable artificial damping technique. The amount of damping in their method is controlled by a parameter called the stencil Reynolds number ($R_{stencil}$).

One Dimensional Simulations

The one dimensional Euler equations are to be used to model the arrangement given in the figure 1. The effectiveness of the IMM solid wall is to be tested with the use of the following initial conditions:

$$p(x, t = 0) = e^{-\ln(2)x^2/25} \quad (7)$$

$$v(x, t = 0) = 0 \quad (8)$$

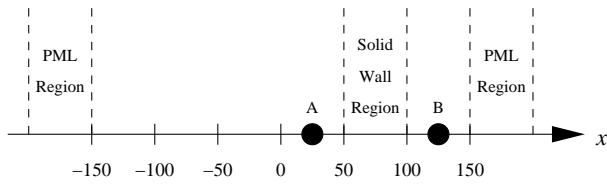


Figure 1: One dimensional arrangement.

Chung and Morris [1] performed an investigation into the IMM in one dimension. They showed that the pressure amplitude of the reflected wave was comparable to that of the incident wave and the transmitted pressure wave had small amplitude. The pressure distribution plot in figure 2 shows results that are almost identical to those obtained by Chung and Morris. Further investigation into the u velocity wave reveals that it is transmitted into the second medium in an amplified form. Plotting the pressure time histories of the points A and B from figure 1 reveals the unexpected results shown in figure 3. This plot shows

that the point in front of the object, point A, has extra pressure waves passing through it. The source of these waves is the pressure wave bouncing around inside the solid wall medium. Behind the solid wall, point B, waves are observed to pass through to this point. These transmitted waves could be eliminated by decreasing the density ratio, however Chung and Morris advise that decreasing the density ratio too much may make the system numerically unstable.

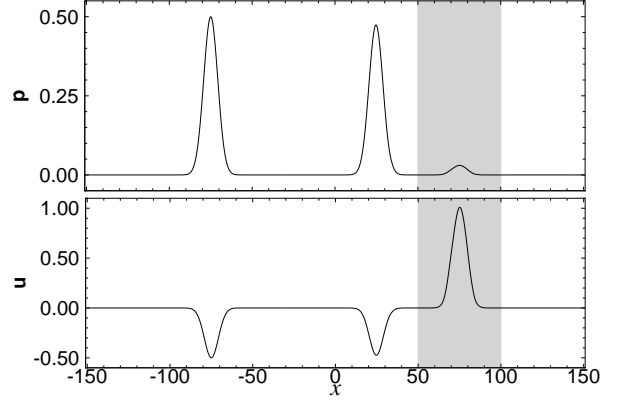


Figure 2: Pressure and velocity at time $t=75$, the reflected and transmitted waves are clearly visible.

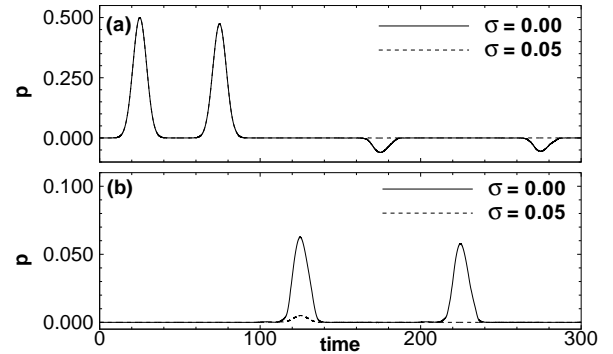


Figure 3: Pressure histories for different values of internal IMM damping (a) Point A in front of the solid object and (b) Point B behind the solid object.

Improvement to the IMM

To prevent the waves bouncing around inside the solid wall region from periodically emitting waves into the rest of the domain, the following damping was added to the governing equations within the solid wall region:

$$\frac{\partial p}{\partial t} = \dots - \sigma p \quad (9)$$

$$\frac{\partial u}{\partial t} = \dots - \sigma u \quad (10)$$

where σ is some damping ratio between zero and one. The experiment was rerun with the extra damping added, the markedly improved results are shown in 3.

Two Dimensional Scattering off a Rectangular Block

In this section acoustic scattering off a rectangular block is to be investigated using the arrangement shown in figure 4. The

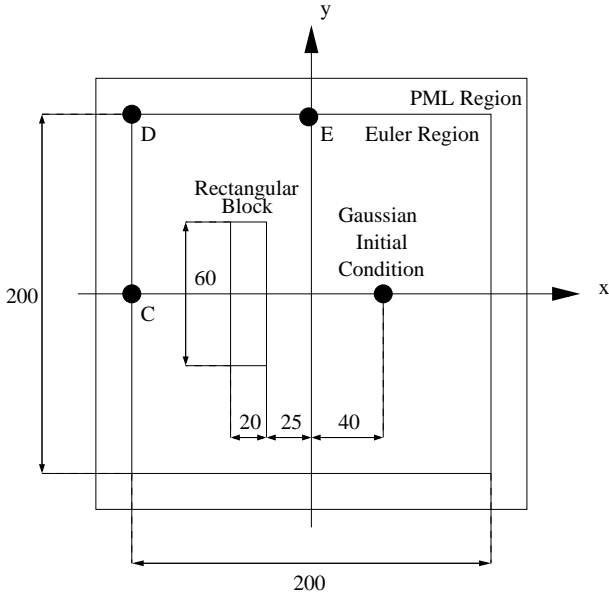


Figure 4: Two dimensional arrangement.

initial condition is to be given by:

$$\rho(x, y, t = 0) = e^{-\ln(2)((x-40)^2+y^2)/3^2} \quad (11)$$

$$u(x, y, t = 0) = 0 \quad (12)$$

$$v(x, y, t = 0) = 0 \quad (13)$$

$$p(x, y, t = 0) = e^{-\ln(2)((x-40)^2+y^2)/3^2} \quad (14)$$

The solid wall boundary was modelled using both the Tam and Dong [7] method and the IMM. The sharp corners of the rectangular object give rise to the development of spurious waves that contaminate the solution. Artificial selective damping will be used to damp these waves, the amount of damping being controlled by the parameter $R_{stencil}$. For the IMM modelling, the parameters that may be adjusted are the density ratio ρ and the IMM internal damping coefficient σ . The test cases to be investigated are given in table 1.

Test Case	Wall Boundary	$R_{stencil}$	IMM ρ	IMM σ
TAM	Tam and Dong	0.1	-	-
IMM1	IMM	0.1	0.030	-
IMM2	IMM	0.1	0.030	0.05
IMM3	IMM	0.1	0.030	0.10
IMM4	IMM	0.1	0.015	0.05
IMM5	IMM	0.2	0.030	0.05

Table 1: Two dimensional test cases.

Results

Using the TAM test case results, contour plots of pressure are shown at different times in figure 7. The block successfully reflects sound off its surface. The pressure histories at point C directly behind the block for several different test cases are shown in figure 5. IMM1 shows poor results without any extra damping inside the block region. IMM2 and IMM3 show how the result is improved as σ is increased. IMM4 shows improvement over IMM2 by having a smaller density ratio. Figure 6 shows the pressure history for point D at the corner of the domain. IMM3 shows marked improvement over IMM1 due to

the addition of damping inside the block region. Finally, figure 8 shows the pressure histories at point E in front of the block. The IMM2 results show high frequency fluctuations in the result. These are due to spurious waves generated when the sound impinges upon the block. These waves may be eliminated by increasing the artificial selective damping coefficient $R_{stencil}$ as shown by IMM5.

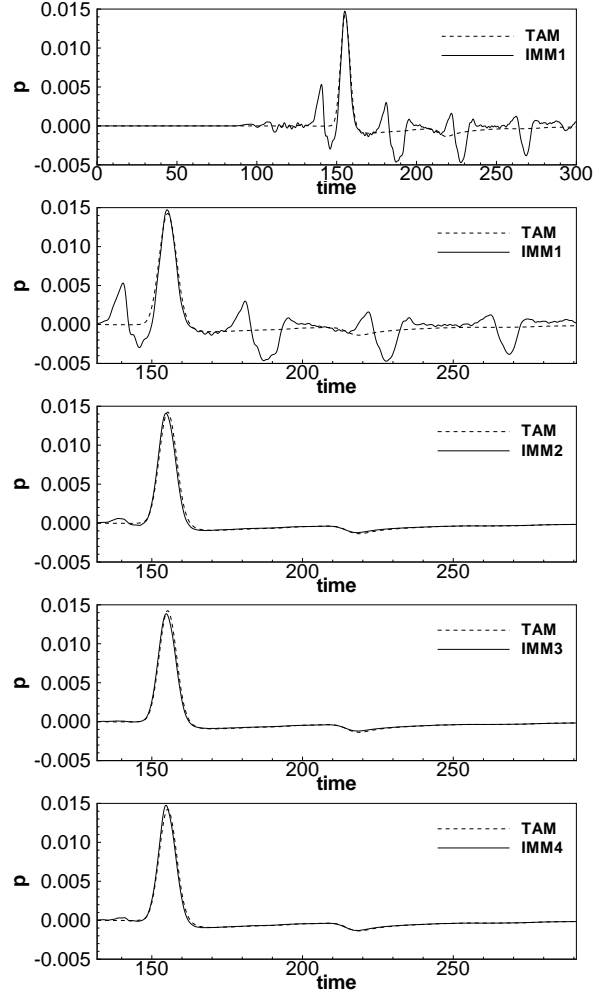


Figure 5: Pressure fluctuations at point C.

Conclusions

An improvement to the Impedance Mismatch Method (IMM) has been suggested for use in both one- and two-dimensional acoustics simulations. This improvement leads to results close to those obtained using the Tam and Dong wall boundary condition.

Acknowledgements

Special thanks to the Defence Science and Technology Organisation for supplying additional funding for this project.

References

- [1] Chung, K. and Morris, P. J. Acoustic Scattering from Two- and Three-Dimensional Bodies, *J. Comput. Acoust.*, **6**, 1998, 357–375.

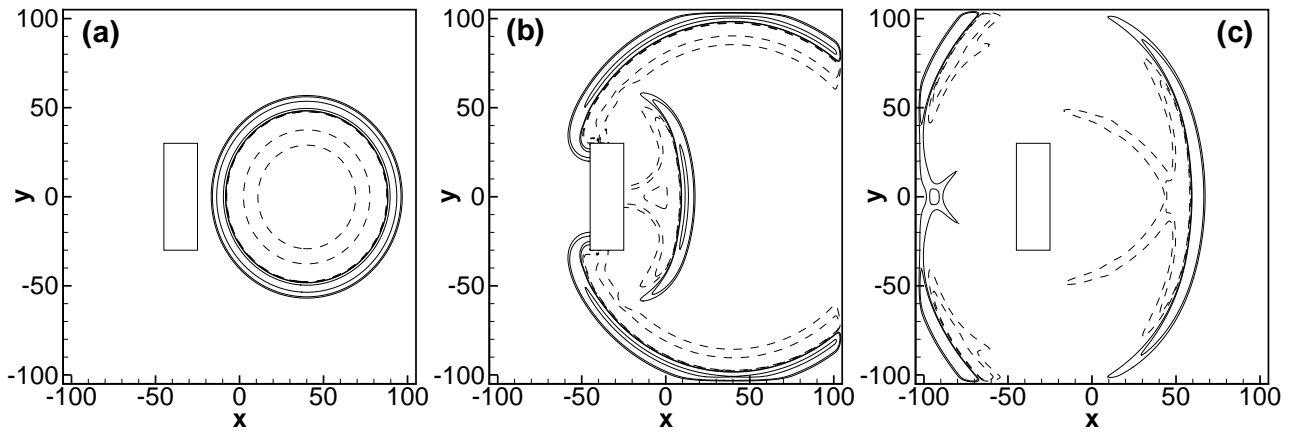


Figure 7: Contours of pressure for the TAM test case (a) $t=50$, (b) $t=100$, (c) $t=150$.

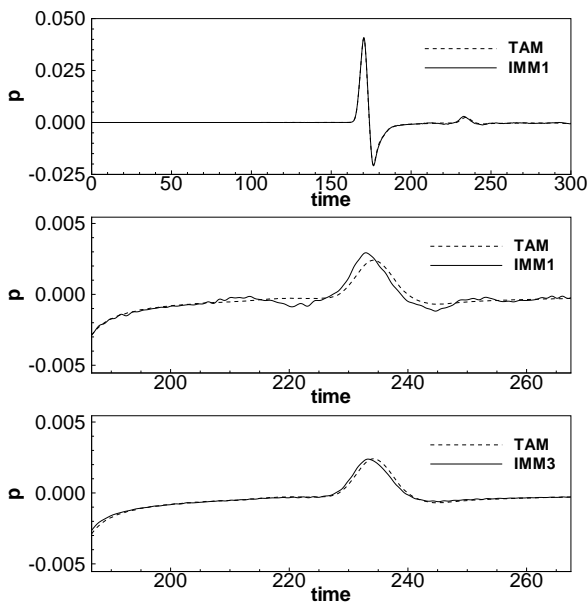


Figure 6: Pressure fluctuations at point D.

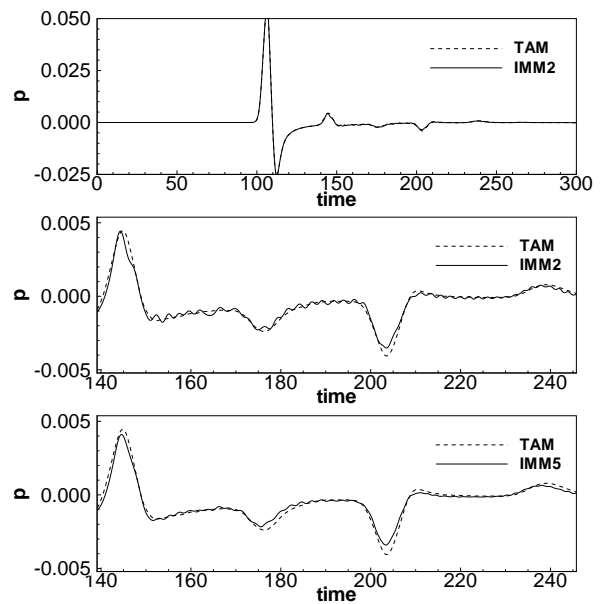


Figure 8: Pressure fluctuations at point E.

- [2] Hu, F.Q., A stable, Perfectly Matched Layer for Linearized Euler Equations in Unsplit Physical Variables, *J. Comput. Phys.*, **173**, 2001, 455–480.
- [3] Hu, F.Q., On Absorbing Boundary Conditions for Linearized Euler Equations By a Perfectly Matched Layer, *J. Comput. Phys.*, **129**, 1996, 201–219.
- [4] Laik, O.A. and Morris, R.J., Direct Simulation of Acoustic Scattering by Two- and Three-Dimensional Bodies, *J. Aircraft*, **37**, 2000, 68–75.
- [5] Tam, C.K.W., Computational Aeroacoustics: Issues and Methods, *AIAA J.*, **33**, 1995, 1788–1796.
- [6] Tam, C.K.W. and Dong, Z., A Study of the Short Wave Components in Computational Acoustics, *J. Comput. Acoust.*, **1**, 1993, 1–30.
- [7] Tam, C.K.W. and Dong, Z., Wall Boundary Conditions for High-Order Finite-Difference Schemes in Computational Aeroacoustics, *Theor. Comput. Fluid Dyn.*, **6**, 1994, 303–322.
- [8] Tam, C.K.W. and Shen, H., Direct Computation of Non-linear Acoustic Pulses Using High Order Finite Difference Schemes, AIAA 93-4325, 15th AIAA Aeroacoustics Conference, 1993.
- [9] Tam, C.K.W. and Webb, J.C., Dispersion-Relation-Preserving Finite Difference Schemes for Computational Acoustics, *J. Comput. Phys.*, **107**, 1993, 262–281.